DOI: 10.1002/chem.200701852

Novel Single-Crystal-to-Single-Crystal Anion Exchange and Self-Assembly of Luminescent d^{10} Metal (Cd^{II}, Zn^{II}, and Cu^{I}) Complexes Containing C_3-Symmetrical Ligands

Biing-Chiau Tzeng,*[a] Tse-Hao Chiu,[a] Bo-So Chen,[a] and Gene-Hsiang Lee[b]

Abstract: Ligands **L1** and **L2′** (**L1** = *N*,*N*′,*N*″-tris(4-pyridyl)trimesic amide, **L2′** = *N*,*N*′,*N*″-tris(3-pyridinyl)-1,3,5-benzenetricarboxamide) belonging to an interesting family of tripyridyltriamides with C_3-symmetry have been utilized to construct 3D porous or hydrogen-bonded frameworks. Through a novel single-crystal-to-single-crystal anion-exchange process, $[Cd(\mathbf{L1})_2(ClO_4)_2]_n$ (**1c**) can be obtained from $[Cd(\mathbf{L1})_2Cl_2]_n$ (**1b**) in the presence of ClO_4^- anions. This anion-exchange process is highly selective and only the substitution of Cl^- by ClO_4^- or PF_6^- could be realized; Cl^- was found not to be substituted by BPh_4^-. This demonstrates that the exchange process depends on the size of the anions in relation to the size of the cavities in the host material (ca. 7.5 Å). In addition, the anion-exchange properties of **1b** have also been investigated by means of powder X-ray diffraction (PXRD), elemental analysis (EA), and infrared absorption spectroscopy (IR). Structurally, $[Zn(\mathbf{L1})(NO_3)_2]_n$ (**2**) consists of a 2D coordination network with five-coordinate Zn^{II} ions. Surprisingly, different trigonal-bipyramidal Zn^{II} ions propagate to form distinct respective sheet structures, **A** and **B**, which are packed in an **A**-**B**-**A**-**B** manner in the crystal lattice, and these are hydrogen-bonded to give a 3D extended framework. The molecular structure of $[CuI(\mathbf{L2'})]_n$ (**3**) shows that the Cu^{I} ion adopts a distorted tetrahedral geometry, and **3** also forms a 2D coordination network. Significantly, this 2D coordination network is further assembled into a remarkable 3D homochiral framework through triple hydrogen bonding and π···π interactions. All of these 3D coordination polymers and/or hydrogen-bonded frameworks are luminescent in the solid state, and their solid-state luminescent properties have been investigated at room temperature and/or at 77 K.

Keywords: anions · hydrogen bonds · luminescence · self-assembly · tripyridyltriamide ligand

Introduction

The coordinative bond approach has been widely used in the construction of supramolecular coordination compounds.[1] Recently, a wide range of 1D, 2D, or 3D infinite solid-state coordination architectures as well as discrete molecular structures have been isolated and structurally characterized,[2] and many of these are anticipated to be potential candidates for molecular materials. Moreover, in parallel, it is possible to use highly directional hydrogen bonds as a means of controlling self-assembly, and thus the simultaneous exploitation of coordinative bonding, hydrogen bonding, and/or other weak interactions has recently been recognized as a very powerful and versatile strategy in supramolecular design and material synthesis.[3] In fact, these structural frameworks have been utilized in applications such as chemical sieving, sensing, and catalysis, and much progress has been made in all of these areas.[4]

Organic amides have proved to be very useful components in self-assembly through hydrogen bonding; moreover, the assembled products have relevance to biological systems. Ghadiri et al.[5] have used cyclic oligoamides as building units to construct interesting nanotubes, resulting in zeolite-like frameworks through inter-ring and/or inter-tube hydrogen bonding. These cyclic oligoamides containing channel structures are anticipated to be a new and important family

[a] Prof. Dr. B.-C. Tzeng, T.-H. Chiu, B.-S. Chen
Department of Chemistry and Biochemistry
National Chung Cheng University
168 University Rd., Min-Hsiung, Chia-Yi, 621 (Taiwan)
Fax: (+886) 5-2721040
E-mail: chebct@ccu.edu.tw

[b] Dr. G.-H. Lee
Instrumentation Center, National Taiwan University
1, Sec. 4, Roosevelt Road, Taipei, 106 (Taiwan)

Supporting information for this article is available on the WWW under http://www.chemeurj.org/ or from the author.

 © 2008 Wiley-VCH Verlag GmbH & Co. KGaA, Weinheim WILEY InterScience DISCOVER SOMETHING GREAT

of molecular materials. On the other hand, related research on metal-containing cyclic amides is still in its infancy. The incorporation of transition metal ions into hydrogen-bonded networks is important because the magnetic and optical characteristics of these ions become part of a broader strategy for crystal engineering of nonlinear optical, conducting, ferromagnetic, and luminescent materials.[3] Puddephatt et al. reported pioneering work based on this novel idea, in which a metal-containing (Pt^{II} ions) molecular triangle was constructed, taking advantage of dipyridylamides (*N*-pyridin-4-yl-isonicotinamide) as bridging ligands and Pt^{II} ions as connectors in the assembly process.[6] This complex cation appears to be a novel example of a cyclic coordination compound that forms a dimeric architecture similar to that formed by cyclic peptides,[5] and it suggests that the biomimetic approach to the organization of coordination networks holds considerable promise.

In 2004, Stang et al. reported an interesting nanoscopic coordination cage, $[Pd_3\mathbf{L1'}_2]^{6+}$ (**L1′** = *N*,*N*′,*N*″-tris(3-pyridyl)-trimesic amide), obtained by self-assembly from Pd^{II} ions and **L1′** ligands, which was characterized by NMR (^{31}P, ^{1}H) and electrospray ionization mass spectrometry.[7] Simulation of the pseudo-trigonal-bipyramidal cages with an MM2 force field showed the cavity diameter to be about 1.9 nm. Later, Lah and co-workers also reported two novel single-crystal structures of the truncated octahedral cages $[Pd_6\mathbf{L1'}_8]^{12+}$ and $[Pd_6\mathbf{L2}_8]^{12+}$ (**L2** = *N*,*N*′,*N*″-tris(4-pyridinyl)-1,3,5-benzenetricarboxamide),[8] and these face-driven corner-linker nanocages were found to have 12 ports at the edge of the truncated octahedron. Lah's work highlights that both the cavity size and the port size of the cage may be controlled by the size of the facial ligands. Very recently, Kitagawa et al. reported the construction of a 3D porous coordination polymer, $[Cd(\mathbf{L1})_2(NO_3)_2]_n$ (**1a**; **L1** = *N*,*N*′,*N*″-tris(4-pyridyl)trimesic amide).[9] The highly ordered amide groups in the channels play an important role in the interaction with guest molecules, which was confirmed by thermogravimetric analysis (TGA), adsorption/desorption measurements, and powder X-ray diffraction studies (PXRD). In addition, catalysis of a Knoevenagel condensation reaction by **1a** demonstrates its reactivity as a selective heterogeneous basic catalyst, interaction with which depends on the sizes of the reactants. The solid catalyst maintains its crystalline framework after the reaction and is easily recycled. Thus, the **L1** and **L2** families show potential as tridentate bridging ligands for the construction of molecular cages or 3D porous coordination polymers, and this offers possibilities for the development of suitable nanosized host systems that can accommodate small molecular guests or catalysts.

We have previously reported the crystal structures and solid-state luminescent properties of 3D $[Cd(\mathbf{L1})_2Cl_2]_n$ (**1b**) and 2D $[Ag(\mathbf{L1'})PF_6]_n$ coordination polymers,[10] with three pyridylamides as functional appendages propagating in the extended structures. In continuation of our efforts in the construction of functional coordination polymers and/or hydrogen-bonded frameworks,[10,11] we report herein on studies of novel single-crystal-to-single-crystal anion exchange and self-assembly of luminescent Cd^{II}, Zn^{II}, and Cu^{I} complexes containing the C_3-symmetrical ligands **L1** and **L2′** (**L2′** = *N*,*N*′,*N*″-tris(3-pyridinyl)-1,3,5-benzenetricarboxamide).

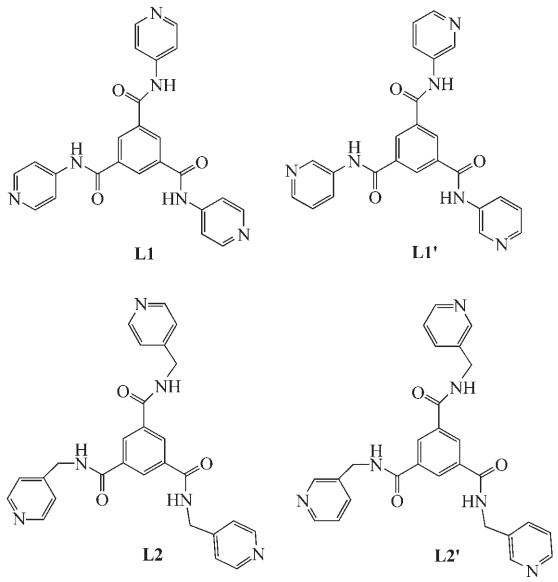

Experimental Section

General information: All solvents for syntheses (analytical grade) were used without further purification, and metal salts (CuI, $Zn(NO_3)_2$, and $Cd(NO_3)_2$) were obtained commercially (Strem Chemicals). **L1**, **L2′**, and $[Cd(\mathbf{L1})_2Cl_2]_n$ (**1b**) were prepared according to literature methods.[10,12]

CAUTION! *Perchlorate salts are potentially explosive and should be handled with care and in small amounts.*

IR spectra were recorded from samples in KBr pellets on a Perkin–Elmer PC 16 FTIR spectrometer, and steady-state emission spectra were recorded on a Hitachi F-7000 spectrophotometer. Thermogravimetric analysis was performed under a flow of air at a heating rate of 10 °C min^{-1} using a Shimadzu TGA-50 system. Powder X-ray diffraction data were recorded on a Shimadzu XRD-6000 diffractometer.

$[Cd(L1)_2X_2]_n$ [X = ClO_4^- (1c), PF_6^- (1d)]: Crystalline samples of **1b** were immersed in a 0.01 M aqueous solution of $LiClO_4$ for 12 h. Although most of the crystals turned opaque, some retained their crystalline properties and were still suitable for X-ray diffraction analysis. **1c** was isolated in about 93% yield. FT-IR (KBr): ν_{NH} = 3240, $\nu_{C=O}$ = 1688, ν_{Cl-O} = 1143, 1120, and 1088 cm^{-1}; elemental analysis calcd (%) for $C_{48}H_{44}CdCl_2N_{12}O_{18}$: C 45.71, H 3.49, N 13.33; found: C 45.74, H 3.88, N 13.65. **1d** was obtained in around 90% yield by a similar method to that described for the synthesis of **1c**, except that NH_4PF_6 was used instead of $LiClO_4$. FT-IR (KBr): ν_{NH} = 3251, $\nu_{C=O}$ = 1682, ν_{P-F} = 828 cm^{-1}; elemental analysis calcd (%) for $C_{48}H_{40}CdF_{12}N_{12}P_2O_8$: C 43.83, H 3.07, N 12.78; found: C 44.27, H 3.29, N 13.08.

$[Zn(L1)(NO_3)_2]_n$ (2): Reaction of **L1** (44 mg, 0.1 mmol) dissolved in MeOH (20 mL) with $Zn(NO_3)_2 \cdot 6H_2O$ (30 mg, 0.1 mmol) at room temperature for 0.5 h gave a white precipitate. Recrystallization of the crude product by diffusion of diethyl ether into a solution in DMF afforded colorless crystals in about 45% yield. FT-IR (KBr): ν_{NH} = 3251, $\nu_{C=O}$ = 1687 cm^{-1}; elemental analysis calcd (%) for $C_{69}H_{89}N_{23}O_{27}Zn_2$: C 45.91, H 4.94, N 17.86; found: C 46.12, H 4.99, N 17.58.

$[CuI(L2')]_n$ (3): CuI (19 mg, 0.1 mmol) dissolved in a saturated methanolic solution of KI (2 mL) was carefully layered onto a solution of **L2′** (48 mg, 0.1 mmol) in DMF (2 mL). After two weeks, pale-yellow crystals

 © 2008 Wiley-VCH Verlag GmbH & Co. KGaA, Weinheim

were obtained in about 64% yield. FT-IR (KBr): $\nu_{NH}=3269$, $\nu_{C=O}=1643\ cm^{-1}$; elemental analysis calcd (%) for $C_{27}H_{24}CuIN_6O_3$: C 48.29, H 3.58, N 12.52; found: C 47.78, H 3.77, N 12.47.

X-ray crystallography: Suitable single crystals of **1c**, **2**, and **3** were each mounted on a glass capillary, and data were collected on a Bruker SMART CCD diffractometer with $Mo_{K\alpha}$ radiation ($\lambda=0.71073$ Å) at 150(2) K. A preliminary orientation matrix and unit-cell parameters were determined from three runs of 15 frames each, each frame corresponding to a scan of 0.3° in 20 s, and this was followed by spot integration and least-squares refinement. Data were collected using an ω scan of 0.3° per frame for 20 s until a complete hemisphere had been covered. Cell parameters were retrieved using SMART[13a] software and refined with SAINT[13b] on all observed reflections. Data reduction was performed with the SAINT software and the resulting data were corrected for Lorentz and polarization effects. Absorption corrections were applied with the program SADABS.[13c] The structures were solved by direct methods with the SHELXS-97[13d] program and refined by full-matrix least-squares methods on F^2 with SHELXL-97.[13e] All non-hydrogen atomic positions were located in difference Fourier maps and refined anisotropically. Hydrogen atoms were constrained to the ideal geometry using an appropriate riding model. Details of the data collection and the refinement of the structures for **1c**·17 H_2O, **2**·H_2O·3.5 DMF, and **3** are summarized in Table 1, and their selected bond distances and angles are summarized in Table 2. Hydrogen bonds in the structures are listed in Table 3.

Table 1. Crystallographic data for **1c**, **2**, and **3**.

	1c·17 H_2O	**2**·H_2O·3.5 DMF	**3**
empirical formula	$C_{48}H_{70}CdCl_2N_{12}O_{31}$	$C_{34.5}H_{44.5}N_{11.5}O_{13.5}Zn$	$C_{27}H_{24}CuIN_6O_3$
M_r	1494.46	901.69	670.96
crystal system	cubic	triclinic	hexagonal
space group (No.)	$Ia\bar{3}$	$P\bar{1}$	$P63$
a [Å]	24.7634(3)	14.6735(7)	14.1457(13)
b [Å]	24.7634(3)	16.9018(9)	14.1457(13)
c [Å]	24.7634(3)	17.1077(9)	7.6098(6)
α [°]	90	91.883(1)	90
β [°]	90	107.244(1)	90
γ [°]	90	91.690(1)	120
V [Å^3], Z	15185.6(3), 8	4046.5(4), 4	1318.7(2), 2
F(000) (e)	6176	1880	668
μ ($Mo_{K\alpha}$) [mm^{-1}]	0.441	0.687	2.040
T [K]	150(2)	150(2)	150(2)
reflections collected	26419	44013	8624
independent reflections ($F_o\geq 2\sigma(F_o)$)	2922 (R_{int}=0.060)	14256 (R_{int}=0.061)	14256 (R_{int}=0.055)
refined parameters	146	1084	1941
GoF on F^2	1.059	1.307	1.124
R[a], R_w[b] ($I\geq 2\sigma(I)$)	0.075, 0.210	0.100, 0.199	0.700, 0.176
R[a], R_w[b] (all data)	0.123, 0.251	0.120, 0.207	0.087, 0.188

[a] $R=\Sigma||F_o|-|F_c||/\Sigma|F_o|$. [b] $wR_2=\{[\Sigma w(F_o^2-F_c^2)^2/\Sigma[w(F_o^2)^2]]\}^{1/2}$.

Table 2. Selected bond lengths [Å] and angles [°] in **1c**, **2**, and **3**.[a]

1c			
Cd(1)–N(1)	2.380(3)	O(1)–C(6)	1.222(5)
N(1)–C(1)	1.329(6)	N(1)–C(5)	1.343(6)
N(2)–C(6)	1.350(6)	N(2)–(3)	1.394(6)
$N(1)^{(1)}$-Cd(1)-$N(1)^{(2)}$	91.82(12)	$N(1)^{(1)}$-Cd(1)-N(1)	180
C(1)-N(1)-C(5)	116.1(4)	C(1)-N(1)-Cd(1)	124.4(3)
C(5)-N(1)-Cd(1)	119.3(3)	C(6)-N(2)-C(3)	128.1(4)
2			
Zn(1)–N(1)	2.056(5)	Zn(2)–N(9)	2.041(5)
Zn(1)–O(7)	2.108(5)	Zn(1)–O(4)	2.158(5)
Zn(2)–O(16)	2.138(5)	Zn(2)–O(13)	2.198(5)
N(1)-Zn(1)-O(7)	91.0(2)	N(1)-Zn(1)-O(4)	86.3(2)
O(7)-Zn(1)-O(4)	163.6(2)	N(9)-Zn(2)-O(16)	90.5(2)
N(9)-Zn(2)-O(13)	87.2(2)	O(16)-Zn(2)-O(13)	161.2(2)
3			
Cu–N(1)	2.066(8)	Cu–I(1)	2.627(3)
$N(1)^{(3)}$-Cu-N(1)	112.6(3)	N(1)-Cu-I(1)	112.6(3)
C(5)-N(1)-Cu	121.9(8)	C(1)-N(1)-Cu	121.4(7)
C(5)-N(1)-C(1)	116.6(9)	C(7)-N(2)-C(6)	124.9(9)

[a] Symmetry positions of atoms : 1) $1-x$, $1-y$, $-z$. 2) $^1/_2+z$, x, $^1/_2-y$. 3) $1-x+y$, $1-x$, z.

Results and Discussion

Recently, we[10] and Kitagawa et al.[9] reported two remarkable examples of 3D coordination polymers of the type $[Cd(\mathbf{L1})_2X_2]_n$ ($X=Cl^-$, NO_3^-), which were shown to display solid-state luminescence, thermal stability, adsorption/desorption properties, and selective heterogeneous size-dependent catalytic activities. To further investigate this intriguing class of porous materials and to study their potential applications, we have now performed anion-exchange studies through a novel crystal-to-crystal process to examine their behavior in relation to the size of the anion. In addition, the assembly process by way of the coordinative bond approach and/or hydrogen bonding has also been studied by treating the C_3-symmetrical ligands (**L1** and **L2′**) with Zn^{II} or Cu^{I} ions, respectively. These 3D coordination polymers and/or hydrogen-bonded frameworks are all air-stable and luminescent in the solid state.

Description of the crystal structures: **1c** crystallized in the $Ia\bar{3}$ space group; its 3D porous framework molecular structure is shown in Figure 1a, which is isostructural with those of **1a** and **1b**. Briefly, the coordination framework is constructed from six-coordinate Cd^{II} ions, each with almost perfect octahedral geometry, and **L1** with pseudo-C_3 symmetry. Furthermore, the two frameworks mutually interpenetrate to give a 3D porous structure with zigzag channels of diameter around 7.5 Å, as shown in Figure 1b. The 3D pores containing tripyridylamide moieties as functional units in the channels are particularly attractive for guest uptake and/or ion-exchange studies, thus making such 3D coordination polymers potentially attractive as molecular materials. In this context, the exchange process was carried out in aqueous solution, and hence the voids were successfully filled with ClO_4^- anions (two, of which one is regularly arranged and the other is disordered) and a large number of water molecules (17 water molecules in an asymmetric unit), which are involved in hydrogen-bonding with the ClO_4^- anions, the amide groups, and even the water molecules themselves in the 3D channels (the hydrogen-bond data are

 © 2008 Wiley-VCH Verlag GmbH & Co. KGaA, Weinheim

Table 3. Hydrogen bonds in the structures of **1c**, **2**, and **3**.

D–H···A [Å]	D–H [Å]	H···A [Å]	D···A [Å]	D–H···A [°]
		1c		
N(2)–H(2A)···O(7)[a]	0.88	2.164	2.937(7)	146.5
O(6)–H(6A)···O(7)	0.89	1.893	2.756(9)	162.6
O(7)–H(7A)···O(2)	0.88	2.555	3.303(7)	143.4
O(8)–H(8A)···O(9)	0.90	1.877	2.680(18)	147.1
		2		
N(2)–H(2A)···O(13)	0.88	2.302	3.152(7)	162.9
N(2)–H(2A)···O(14)	0.88	2.434	3.088(8)	131.6
N(4)–H(4A)···O(22)	0.88	2.100	2.968(8)	168.8
N(6)–H(6B)···O(23)[b]	0.88	2.053	2.908(8)	164.1
N(10)–H(10A)···O(5)	0.88	2.186	3.005(8)	154.9
N(12)–H(12A)···O(24)	0.88	1.960	2.824(7)	166.5
N(14)–H(14A)···O(20)	0.88	1.989	2.838(7)	161.6
O(16)–H(16A)···O(10)[c]	0.90	1.881	2.741(7)	159.8
O(16)–H(16B)···O(27)	0.90	1.768	2.641(8)	162.8
O(27)–H(27)···O(17)	0.90	1.910	2.802(10)	170.1
O(27)–H(27′)···O(26)[d]	0.90	1.851	2.743(11)	170.9
		3		
N(2)–H(2)···O(1)[e]	0.88	2.379	3.129(17)	143.5

Symmetry positions of atoms: [a] x, $1/2-y$, $-1/2+z$; $ab=2$. [b] $-1+x$, y, $-1+z$. [c] $2-x$, $2-y$, $1-z$. [d] $1-x$, $2-y$, $1-z$. [e] $x-y$, x, $-1/2+z$.

shown in Table 3). It is noted that the formation of **1c** represents a rare and remarkable example of a successful single-crystal-to-single-crystal anion-exchange process,[1b] suggesting that **1b** has a robust structural framework.

Complex **2** crystallized in the $P\bar{1}$ space group. The molecular structures in Figure 2a and b show that the Zn^{II} ions adopt a distorted trigonal-bipyramidal geometry, where the structure in Figure 2a is composed of three nitrogen atoms from three different tridentate bridging **L1** ligands and two *trans* terminal NO_3^- anions, and that in Figure 2b contains three nitrogen atoms from three **L1** ligands, one coordinated NO_3^- anion, and one water molecule. Such a connection mode in combination with tridentate-bridging **L1** makes **2** a regular 2D coordination network. Surprisingly, different trigonal-bipyramidal Zn^{II} ions propagate in their respective sheet structures, with **A** (Figure 2a) and **B** (Figure 2b) packed in an **A**-**B**-**A**-**B** manner in the crystal lattice. The **A** and **B** sheets are hydrogen-bonded through coordinated NO_3^-···amide interactions [N(10)···O(5) 3.005(8) Å, and (doubly) N(2)···O(13) 3.152(7) Å and N(2)···O(14) 3.088(8) Å]. The dimeric sheet structures shown in Figure 2c are further hydrogen-bonded through coordinated water···amide interactions [O(16)···O(10) 2.741(7) Å] to give a 3D extended framework, as shown in Figure 2d. Thus, the porous framework of **2** is filled with free NO_3^- ions and water and DMF molecules. Significantly, the huge 48-membered macrocycles constructed from three five-coordinate Zn^{II} ions as connectors and three pyridylamide moieties as bridges propagate to form the 2D extended structures, and indeed the structural motif is reminiscent of the framework of $[Ag(\mathbf{L1})(PF_6)]_n$,[10] in which three trigonal Ag^I ions and three tripyridylamide moieties constitute the 48-membered macrocycles. Although five-coordinate Zn^{II} ions are not uncommon, the fact that two different geometric configurations of Zn^{II} ions lead to distinct respective sheet structures in the crystal lattice is interesting. We reason that the trigonal-bipyramidal geometries in **2** seem to be correlated with the steric hindrance from the NO_3^- anions.

The molecular structure of **3**, which crystallized in the $P6_3$ space group, is shown in Figure 3a. The Cu^I ion adopts a distorted tetrahedral geometry, which is composed of three nitrogen atoms from three different tridentate bridging **L2′** ligands and one terminal iodide. The C_3 axis passes through the Cu^I center and iodine atom (the distance between neighboring Cu^I···I axes in the crystal lattice is 4.980 Å), and such a connection mode in combination with tridentate bridging **L2′** ligands also makes **3** a regular 2D coordination network, as shown in Figure 3b. In addition, the huge 48-membered macrocycles constructed from three four-coordinate Cu^I ions as connectors and three pyridylamide moieties as bridges propagate to form the 2D extended structure, which is similar to those of **2** and $[Ag(\mathbf{L1})(PF_6)]_n$.[10] Significantly, this 2D coordination network is further assembled into a remarkable 3D extended framework through triple hydrogen bonding [N(2)···O(1) 3.129(17) Å] and π···π interactions (centroid··· centroid distance of phenyl rings: 3.805 Å), as shown in Figure 3c, and this triple-hydrogen-bonding motif represents a novel example of a triple helix. Indeed, the refined absolute Flack factor is 0.15(7). Moreover, we also refined the data using racemic twin refinement for **3**, and this did not lead to significant improvements in the results. After examining the asymmetric unit of the crystal structure, we could rule out the possibility of a racemic mixture growing in one crystal. This indicates that the absolute configuration in the present case is most likely to be homochiral.

In this study, it was interesting to find that upon reaction with 4-pyridyltriamides (**L1**) or 3-pyridyltriamides (**L2′**), the different d^{10} metal ions (Cd^{II}, Zn^{II}, and Cu^I) generate structural motifs that dramatically change from 2D coordination polymers (**2** and **3**) to 3D coordination polymers (**1c**). Moreover, **2** and **3** are further hydrogen-bonded to form 3D frameworks, in which two different geometric compositions of five-coordinate Zn^{II} ions are found in the respective sheet structures for **2**, and a novel hydrogen-bonded motif, namely a triple helical hydrogen bond, is observed for **3**. In addition, a systematic change in the coordination geometries of the metal ions from tetrahedral (four-coordinate) Cu^I ions to trigonal-bipyramidal (five-coordinate) Zn^{II} ions to octahedral (six-coordinate) Cd^{II} ions has been observed, leading to the different structural frameworks.

 © 2008 Wiley-VCH Verlag GmbH & Co. KGaA, Weinheim

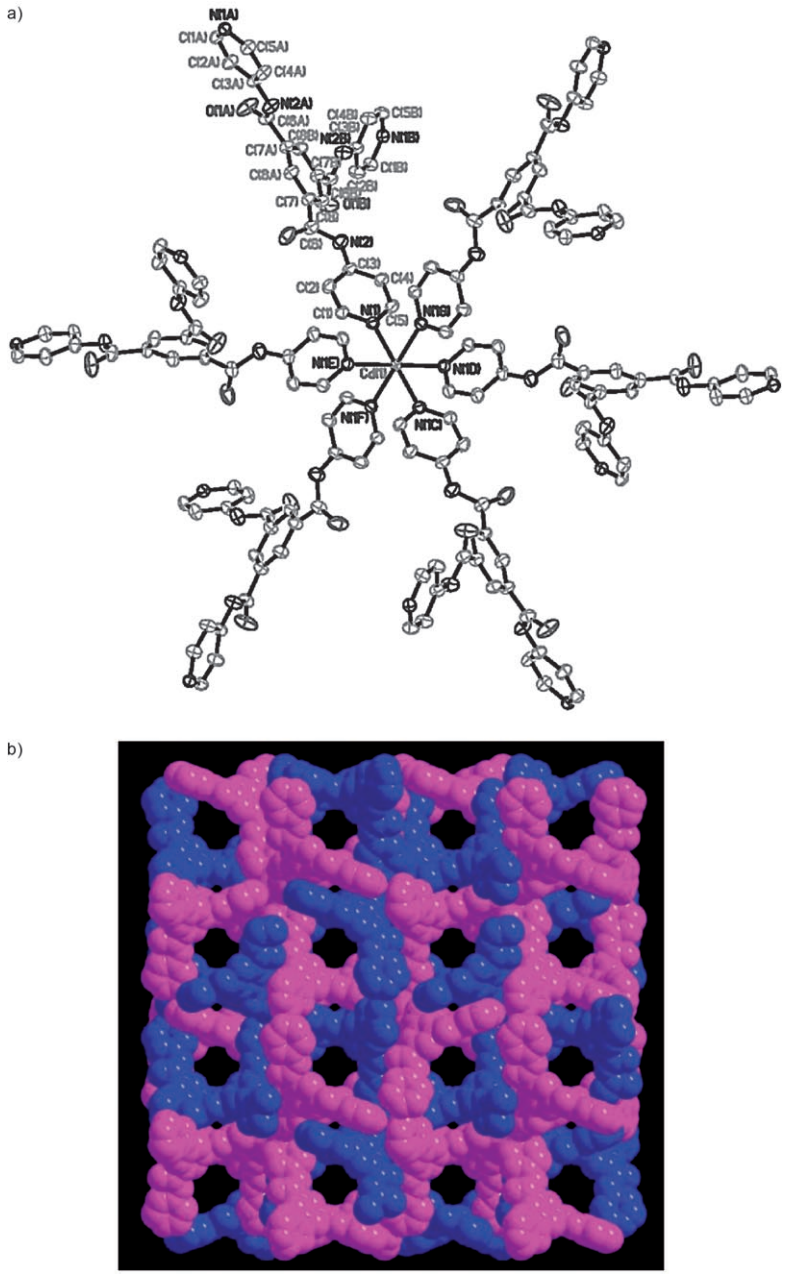

Figure 1. a) Molecular structure of **1c** as an ORTEP representation showing 50% probability ellipsoids, and b) space-filling model of two frameworks mutually interpenetrated to give 3D porous and zigzag channels.

Thermogravimetric analysis and powder X-ray diffraction studies: To examine the thermal stabilities of the compounds, **1c** and **3** were subjected the TGA and PXRD analysis. The weight loss from **1c** was found to be 18.4% upon heating a solid sample to 320°C, which is roughly consistent with the calculated weight loss of 20.5% for seventeen water molecules. Above this temperature, **1c** starts to decompose. Indeed, the decomposition temperature of 320°C is higher than those of **1a** (260°C) and **1b** (250°C), suggesting that **1c** has greater thermal stability. The reason for this could lie in the bulkiness of ClO_4^- compared with NO_3^- and Cl^-, which results in there being less void space in the crystal lattice of **1c**. For **3**, there are no solvating molecules in the crystal lattice, and it is thermally stable up to 330°C. In contrast to the 3D coordination polymer structure of **1c**, **3** has a 3D chiral hydrogen-bonded framework, and hence we reason that its thermal stability may be ascribed to the triple-helical hydrogen bonding in the solid-state structure. The PXRD patterns recorded for solid samples of **1c** and **3** at room temperature closely resemble the simulated patterns (based on the single-crystal data), suggesting good thermal stability of the crystal lattice. Moreover, the structural framework of **1c** remains unchanged following the loss of water, further corroborating its robust nature. The TGA and PXRD results clearly indicate that the triple-hydrogen-bonding motif in **3** enhances the thermal stability of this compound compared to the 3D coordination polymers (**1a–c**).

Solid-state emission spectra: **L1**, **L2′**, and their respective complexes are all luminescent in the solid state, and their emission spectra measured from solid samples are shown in Figure 4. Upon photoexcitation at 300–350 nm, **L1** shows an emission with a maximum at around 467 nm at room temperature, whereas **1b–d** each display a broad and low-energy emission at about 513, 511, and 505 nm, respectively, with in each case a high-energy shoulder in the region 435–465 nm. Given that there is a significant red shift on going from **L1** to **1b–d**, the low-energy emissions in the region 505–513 nm are unlikely to originate purely from **L1** itself (intraligand transition, IL). With reference to our previous study,[10,11c] this low-energy emission could be tentatively assigned to a metal-to-ligand charge-transfer (MLCT) transition, possibly mixed with an IL transition. In fact, these low-energy emissions in the region 505–513 nm for **1b–d** also suggest that the anions do not have any significant effect on the emission properties. The high-energy emissions are quite similar to that of **L1**, and they are most likely due to an IL transition.

 © 2008 Wiley-VCH Verlag GmbH & Co. KGaA, Weinheim

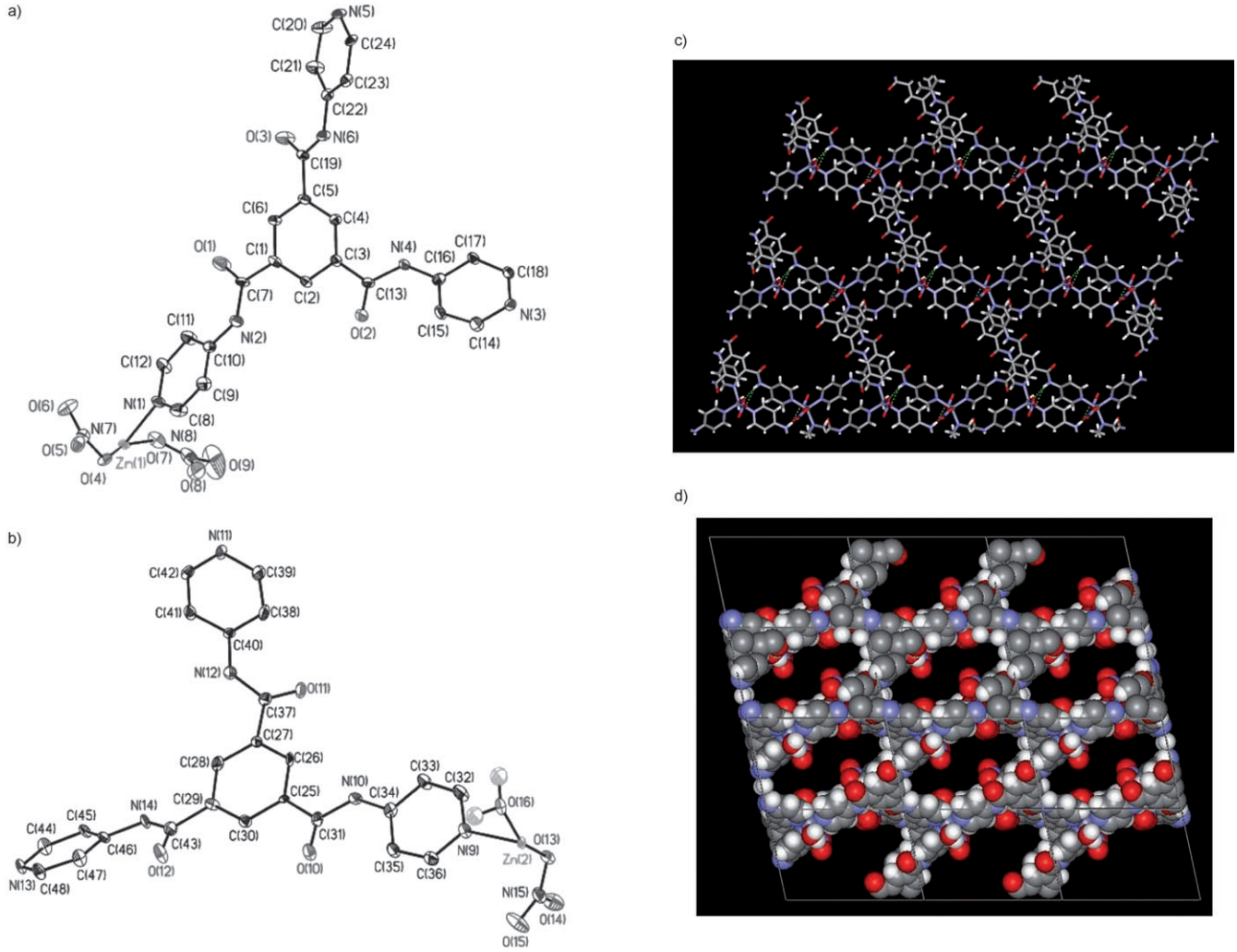

Figure 2. a) Molecular structure of **2** (**A**) containing a trigonal-bipyramidal Zn^{II} ion with two *trans* terminal NO_3^- anions as an ORTEP representation showing 50% probability ellipsoids, b) molecular structure of **2** (**B**) containing a trigonal-bipyramidal Zn^{II} ion coordinated by a *trans* NO_3^- anion and a water molecule as an ORTEP representation showing 50% probability ellipsoids, c) the hydrogen-bonded dimer of sheet structures **2** (**A**) and **2** (**B**), and d) a 3D hydrogen-bonded framework of **2**.

The emission for **2** is centered at about 460 nm, and an IL origin is thus suggested due to an almost exact overlap with that of **L1** (Figure 4a).

Solid samples of **L2′** show a high-energy emission with a maximum at about 428 nm upon photoexcitation at 300–350 nm at room temperature, and **3** displays a low-energy emission at around 512 nm (Figure 4b). Given that there is a significant red shift on going from **L2′** to **3**, this low-energy emission of **3** is most likely to have originated from an I-to-Cu^I charge-transfer (ligand-to-ligand charge-transfer) transition, based on the strong σ-donating strength of iodide, our previous assignments for $[ZnI_2(\mathbf{L})]_2$ (**L**=*N*,*N*′-bis-4-methylpyridyl oxalamide),[11a] and other reports.[14] Upon cooling to 77 K, the emission is red-shifted to about 536 nm, and this unusual red shift is consistent with recent observations on [CuX(2,3-dimethylpyrazine)] (X=Cl, Br, I) reported by Näther et al., for which a similar LLCT assignment was made.[15]

Anion-exchange studies: The anion-exchange properties of **1b** were investigated by means of powder and single-crystal X-ray diffraction analysis, elemental analysis, and infrared absorption spectroscopy. The results showed that immersion of crystals of **1b** in a 0.01 M aqueous solution of $LiClO_4$ or NH_4PF_6 for 12 h led to complete replacement of Cl^- by ClO_4^- or PF_6^-, respectively. The IR spectrum of **1c** shows a new and intense ClO_4^- band in the region 1143–1088 cm^{-1}, and that of **1d** shows a new and intense PF_6^- band at 828 cm^{-1}. Other peaks in the spectra remain virtually unchanged, suggesting that the skeletal structure of the complexes remains intact after the exchange process, as shown in Figure 5. The peaks in the PXRD patterns of the exchanged complexes **1c** and **1d** are almost the same as in that of **1b**, indicating that the crystalline framework remains unchanged. Elemental analyses of the exchanged samples confirmed the compositions of **1c** and **1d** (see the Experimental Section), thus further corroborating that complete

 © 2008 Wiley-VCH Verlag GmbH & Co. KGaA, Weinheim

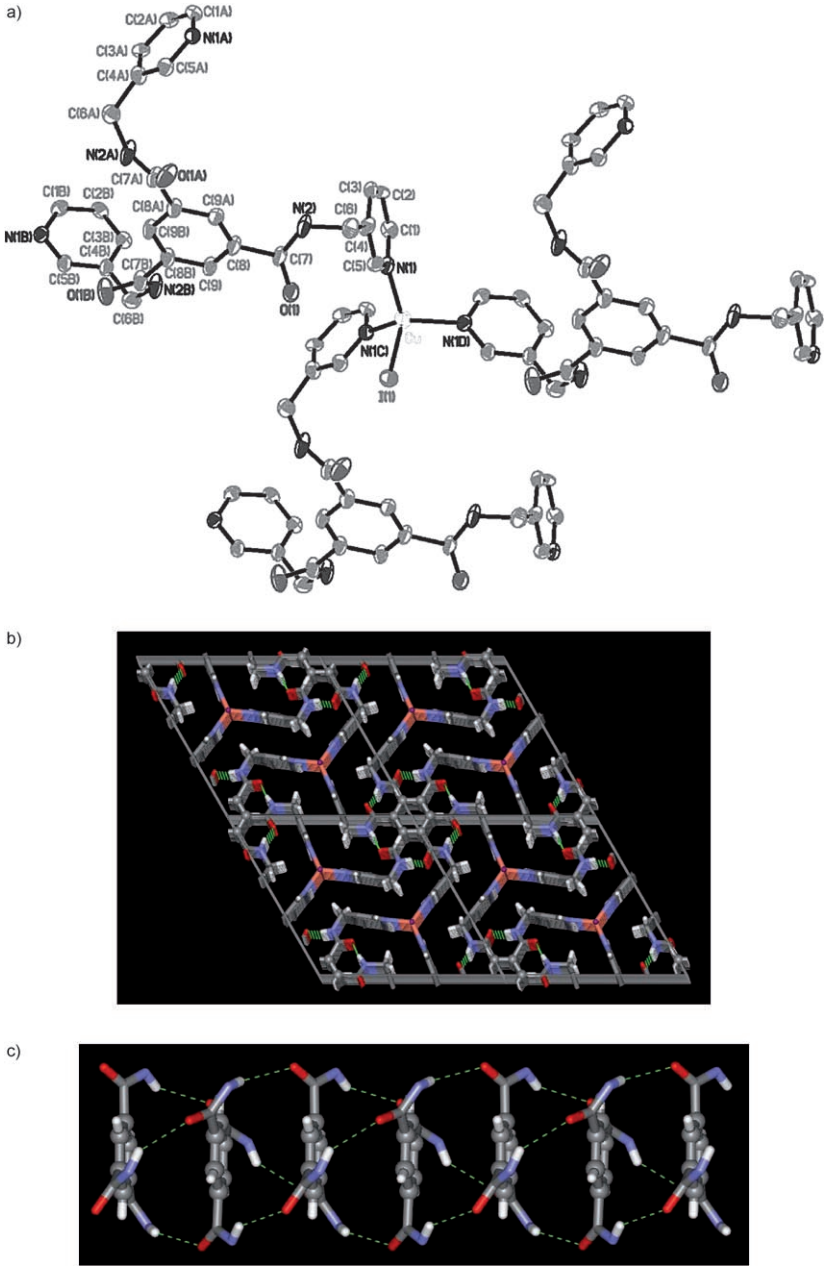

Figure 3. a) Molecular structure of **3** as an ORTEP representation showing 50% probability ellipsoids, b) the 2D coordination network, and c) triple hydrogen-bonding and π···π interactions within a 3D hydrogen-bonded framework.

anion exchange had taken place. Notably, anion exchange of **1b** was found to be highly selective; only the substitution of Cl^- by ClO_4^- or PF_6^- was achieved, whereas attempted anion exchange of Cl^- with BPh_4^- proved unsuccessful. This demonstrates that the exchange process depends on the size of the anion. The diameters of ClO_4^-, PF_6^-, and BPh_4^- are calculated to be approximately 3.8, 3.4, and 8.7 Å, respectively, and thus it would seem that the anion exchange is closely related to the size of the cavities in **1b** (ca. 7.5 Å) compared to the sizes of the various anions. Surprisingly, **1c** can be isolated from **1b** in the presence of ClO_4^- anions through a novel single-crystal-to-single-crystal exchange process. Its molecular structure was also determined by single-crystal X-ray diffraction analysis, and the results suggest that the structural framework of **1b** is quite robust.

Conclusion

Ligands **L1** and **L2′** belonging to an interesting family of tripyridyltriamides with C_3-symmetry have been utilized to coordinate Cd^{II}, Zn^{II}, and Cu^{I} ions in a tridentate bridging manner, leading to the formation of 3D porous or hydrogen-bonded frameworks, respectively. Through a novel single-crystal-to-single-crystal anion-exchange process, **1c** can be isolated from **1b** in the presence of ClO_4^- anions. Its 3D porous network containing tripyridylamide moieties as functional units in the pores and zigzag channels of diameter around 7.5 Å is isostructural with those of **1a** and **1b**. This anion-exchange process is highly selective and only the substitution of Cl^- by ClO_4^- and PF_6^- could be realized; attempted substitution by BPh_4^- did not occur. This demonstrates that the exchange process depends on the size of the anion in relation to the size of the cavities in the host material. Additionally, the anion-exchange properties of **1b** have also been investigated by means of powder X-ray diffraction analysis, elemental analysis, and infrared absorption spectroscopy. Structurally, **2** forms a 2D coordination network with five-coordinate Zn^{II} ions. Surprisingly, different trigonal-bipyramidal Zn^{II} ions propagate in the respective sheet structures, which are packed in an **A**-**B**-**A**-**B** manner in the crystal lattice, and these layers are hydrogen-bonded to give a 3D extended framework. The molecular structure of **3** shows that the Cu^{I} ion adopts a distorted tetrahedral geometry, and such a connection mode in combination with tridentate bridging **L2′** ligands makes **3** a regular 2D coordination network. Significantly, this 2D coordination network is further assembled into a remarkable 3D

 © 2008 Wiley-VCH Verlag GmbH & Co. KGaA, Weinheim

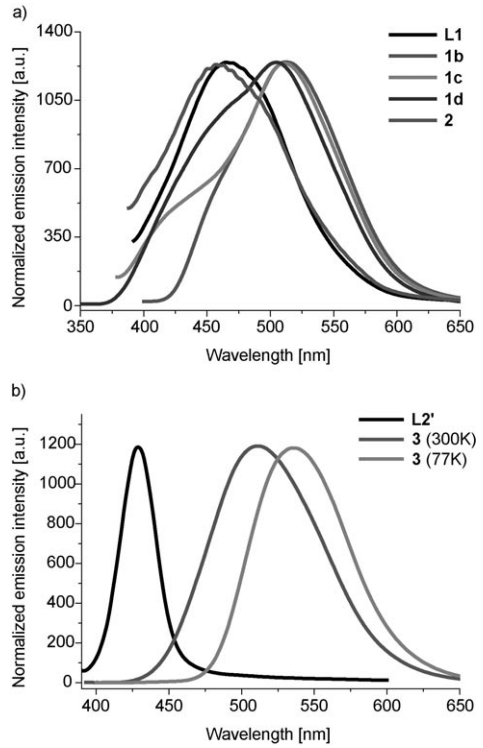

Figure 4. a) Solid-state emission spectra of **L1**, **1b–d**, and **2** at room temperature, and b) the solid-state emission spectra of **L2′** and **3** at room temperature and at 77 K. Excitation wavelengths were 300–350 nm.

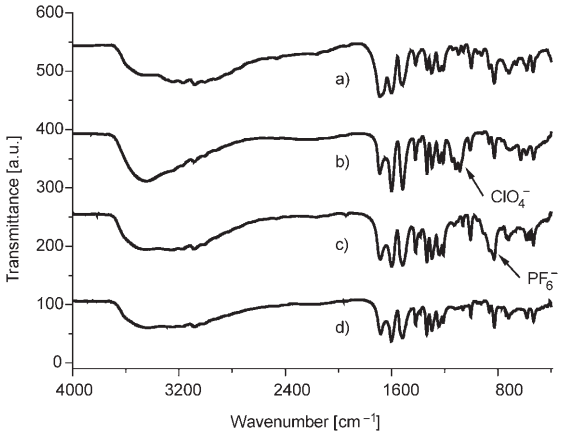

Figure 5. IR (KBr pellet) spectra of **1b** a) as prepared, b) after exchange with $LiClO_4$, c) after exchange with NH_4PF_6, and d) after exchange with $NaBPh_4$.

homochiral framework through triple hydrogen bonding and π···π interactions. To examine their thermal stabilities, **1c** and **3** were subjected to TGA and PXRD analysis. Both the 3D coordination polymer and hydrogen-bonded framework showed thermal stability at up to 320–330 °C. This thermal stability may be ascribed to the contribution of the triple-helical hydrogen bonds.

These 3D coordination polymer and hydrogen-bonded frameworks are all luminescent in the solid state. **1b–d** display low-energy and broad emissions at around 505–513 nm, and with reference to our previous study, this low-energy emission could be tentatively assigned to an MLCT transition, possibly mixed with an IL transition. The emission of **2** is centered at about 460 nm, an IL origin for which is suggested by an almost exact overlap with that of **L1**. Given that there is a significant red shift on going from **L2′** to **3**, the low-energy emission of **3** at around 512 nm is most likely to originate from an I-to-Cu^I charge-transfer transition, based on the strong σ-donating strength of iodide and previous reports.[11a,14,15]

Acknowledgement

We thank the National Science Council and National Chung Cheng University of the Republic of China for financial support.

[1] a) C. Janiak, *Dalton Trans.* **2003**, 2781; b) O. M. Yaghi, H. Li, C. Davis, D. Richardson, T. L. Groy, *Acc. Chem. Res.* **1998**, *31*, 474; c) G. F. Swiegers, T. J. Malefetse, *Chem. Rev.* **2000**, *100*, 3483; d) M. J. Zaworotko, *Angew. Chem.* **2000**, *112*, 3180; *Angew. Chem. Int. Ed.* **2000**, *39*, 3052; e) S. R. Batten, R. Robson, *Angew. Chem.* **1998**, *110*, 1558; f) P. J. Hagrman, D. Hagrman, J. Zubieta, *Angew. Chem.* **1999**, *111*, 2798; *Angew. Chem. Int. Ed.* **1999**, *38*, 2639; g) S. L. James, *Chem. Soc. Rev.* **2003**, *32*, 276; h) S. Kitagawa, R. Kitaura, S.-I. Noro, *Angew. Chem.* **2004**, *116*, 2388; *Angew. Chem. Int. Ed.* **2004**, *43*, 2334.

[2] a) M. Fujita, *Chem. Soc. Rev.* **1998**, *27*, 417; b) S. Leininger, B. Olenyuk, P. J. Stang, *Chem. Rev.* **2000**, *100*, 853; c) B. J. Holliday, C. A. Mirkin, *Angew. Chem.* **2001**, *113*, 2076; *Angew. Chem. Int. Ed.* **2001**, *40*, 2022; d) P. H. Dinolfom, J. T. Hupp, *Chem. Mater.* **2001**, *13*, 3113; e) S. R. Seidel, P. J. Stang, *Acc. Chem. Res.* **2002**, *35*, 972; f) M. Fujita, M. Tominaga, A. Hori, B. Therrien, *Acc. Chem. Res.* **2005**, *38*, 371; g) P. Thanasekaran, R.-T. Liao, Y.-H. Liu, T. Rajendran, S. Rajagopal, K.-L. Lu, *Coord. Chem. Rev.* **2005**, *249*, 1085; h) J. L. Atwood, L. J. Barbour, *Cryst. Growth Des.* **2003**, *3*, 3; i) F. A. Cotton, C. Lin, C. A. Murillo, *Acc. Chem. Res.* **2001**, *34*, 759; j) P. J. Steel, *Acc. Chem. Res.* **2005**, *38*, 243.

[3] a) A. D. Burrows, C.-W. Chan, M. W. Chowdhry, J. E. McGrady, D. M. P. Mingos, *Chem. Soc. Rev.* **1995**, *24*, 329; b) N. C. Gianneschi, E. R. T. Tiekink, L. M. Rendina, *J. Am. Chem. Soc.* **2000**, *122*, 8474; c) A. D. Burrows, D. M. P. Mingos, A. J. P. White, D. J. Williams, *Chem. Commun.* **1996**, 97; d) Z.-N. Chen, H.-X. Zhang, K.-B. Yu, K.-C. Zheng, H. Cai, B.-S. Kang, *J. Chem. Soc. Dalton Trans.* **1998**, 1133; e) C. B. Aakeröy, A. M. Beatty, B. A. Helfrich, *J. Chem. Soc. Dalton Trans.* **1998**, 1943; f) B. R. Cameron, S. S. Corrent, S. J. Loeb, *Angew. Chem.* **1995**, *107*, 2900; *Angew. Chem. Int. Ed. Engl.* **1995**, *34*, 2689; g) S. B. Copp, S. Subramanian, M. J. Zaworotko, *J. Am. Chem. Soc.* **1992**, *114*, 8719; h) Z. Qin, M. C. Jennings, R. J. Puddephatt, *Chem. Commun.* **2002**, 354; i) S. Muthu, J. H. K. Yip, J. J. Vittal, *J. Chem. Soc. Dalton Trans.* **2002**, 4561; j) S. Muthu, J. H. K. Yip, J. J. Vittal, *J. Chem. Soc. Dalton Trans.* **2001**, 3577; k) T. J. Burchell, D. J. Eisler, R. J. Puddephatt, *Inorg. Chem.* **2004**, *43*, 5550; l) C. L. Schauer, E. Matwey, F. W. Fowler, J. W. Lauher, *Cryst. Eng.* **1998**, *1*, 213.

[4] a) S. Bélanger, J. T. Hupp, C. L. Stern, R. V. Slone, D. F. Watson, T. M. Carrell, *J. Am. Chem. Soc.* **1999**, *121*, 557; b) S. Bélanger, J. T. Hupp, *Angew. Chem.* **1999**, *111*, 2360; *Angew. Chem. Int. Ed.* **1999**, *38*, 2222; c) G. A. Mines, B.-C. Tzeng, K. J. Stevenson, J. Li, J. T. Hupp, *Angew. Chem.* **2002**, *114*, 162; *Angew. Chem. Int. Ed.* **2002**, *41*, 154; d) M. H. Keefe, R. V. Slone, J. T. Hupp, K. F. Czaplewski, R. Q. Snurr, C. L. Stern, *Langmuir* **2000**, *16*, 3964; e) M. L. Merlau, M. d. P. Mejia, S. T. Nguyen, J. T. Hupp, *Angew. Chem.* **2001**, *113*, 4369; *Angew. Chem. Int. Ed.* **2001**, *40*, 4239; f) S. Tashiro, M. Tominaga, M. Kawano, B. Therrien, T. Ozeki, M. Fujita, *J. Am. Chem.*

 © 2008 Wiley-VCH Verlag GmbH & Co. KGaA, Weinheim

Soc. **2005**, *127*, 4546; g) M. Yoshizawa, Y. Takeyama, T. Okano, M. Fujita, *J. Am. Chem. Soc.* **2003**, *125*, 3243.

[5] a) J. D. Hartgerink, T. D. Clark, M. R. Ghadiri, *Chem. Eur. J.* **1998**, *4*, 1367; b) M. R. Ghadiri, K. Kobayashi, J. R. Granja, R. K. Chadha, D. E. McRee, *Angew. Chem.* **1995**, *107*, 76; *Angew. Chem. Int. Ed. Engl.* **1995**, *34*, 93.

[6] a) Z. Qin, M. C. Jennings, R. J. Puddephatt, *Chem. Commun.* **2001**, 2676; b) Z. Qin, M. C. Jennings, R. J. Puddephatt, *Inorg. Chem.* **2003**, *42*, 1956.

[7] P. S. Mukherjee, N. Das, P. J. Stang, *J. Org. Chem.* **2004**, *69*, 3526.

[8] D. Moon, S. Kang, J. Park, K. Lee, R. P. John, H. Won, G. H. Seong, Y. S. Kim, G. H. Kim, H. Rhee, M. S. Lah, *J. Am. Chem. Soc.* **2006**, *128*, 3530.

[9] S. Hasegawa, S. Horike, R. Matsuda, S. Furukawa, K. Mochizuki, Y. Kinoshita, S. Kitagawa, *J. Am. Chem. Soc.* **2007**, *129*, 2607.

[10] B.-C. Tzeng, B.-S. Chen, H.-T. Yeh, G.-H. Lee, S.-M. Peng, *New J. Chem.* **2006**, *30*, 1087.

[11] a) B.-C. Tzeng, B.-S. Chen, S.-Y. Lee, W.-H. Liu, G.-H. Lee, S.-M. Peng, *New J. Chem.* **2005**, *29*, 1254; b) B.-C. Tzeng, H.-T. Yeh, Y.-L. Wu, J.-H. Kuo, G.-H. Lee, S.-M. Peng, *Inorg. Chem.* **2006**, *45*, 591; c) B.-C. Tzeng, Y.-M. Lu, G.-H. Lee, S.-M. Peng, *Eur. J. Inorg. Chem.* **2006**, 1698; d) B.-C. Tzeng, Y.-C. Huang, B.-S. Chen, W.-M. Wu, S.-Y. Lee, G.-H. Lee, S.-M. Peng, *Inorg. Chem.* **2007**, *46*, 186; e) B.-C. Tzeng, Y.-F. Chen, C.-C. Wu, C.-C. Hu, Y.-T. Chang, C.-K. Chen, *New J. Chem.* **2007**, *31*, 202.

[12] J. Fan, H.-F. Zhu, T. A. Okamura, W.-Y. Sun, W.-X. Tang, N. Ueyama, *Chem. Eur. J.* **2003**, *9*, 4724.

[13] a) *SMART V5.625 Software for the CCD Detector System*, Bruker-AXS Instruments Division, Madison, WI, **2000**; b) *SAINT V6.22*, *Software for the CCD Detector System*, Bruker-AXS Instruments Division, Madison, WI, **2000**; c) G. M. Sheldrick, *SADABS*, V 2.03, University of Göttingen, Germany, **2002**; d) G. M. Sheldrick, SHELXS-97, *Acta Crystallogr. Sect. A* **1990**, *46*, 467; e) G. M. Sheldrick, SHELXL-97, University of Göttingen (Germany), **1997**.

[14] a) K. A. Truesdell, G. A. Crosby, *J. Am. Chem. Soc.* **1985**, *107*, 1787; b) G. A. Crosby, R. G. Highland, K. A. Truesdell, *Coord. Chem. Rev.* **1985**, *64*, 41.

[15] I. Jeß, P. Taborsky, J. Pospíšil, C. Näther, *Dalton Trans.* **2007**, 2263.

Received: November 25, 2007
Revised: February 22, 2008
Published online: April 18, 2008

 © 2008 Wiley-VCH Verlag GmbH & Co. KGaA, Weinheim